

Supporting Information

for

C–C and C–O Bond Formation Reactivity of Nickel Complexes Supported by the Pyridinophane $^{\text{Me}}\text{N}_3\text{C}$ Ligand

Joshua Ji-Nung Leung,^{1,‡} Dae Young Bae,^{1,‡} Yusuff Moshhood,^{1,‡} Liviu M. Mirica^{1,*}

Department of Chemistry, University of Illinois at Urbana-Champaign, 600 S. Mathews Avenue,
Urbana, Illinois, 61801, United States.

* corresponding author: mirica@illinois.edu

‡ these authors contributed equally

Table of Contents

I. General Specifications.....	S2
II. Experimental Details	S3
III. Reactivity Studies	S8
IV. UV-Vis Spectra.....	S11
V. Cyclic Voltammograms	S14
VI. Computational Details	S16
VII. X-ray Structure Determinations	S188
VIII. References.....	S38

I. General Specifications

All manipulations are carried out under an inert atmosphere using a nitrogen-filled glovebox or standard Schlenk techniques unless otherwise noted. All reagents for which synthesis is not given are commercially available from Sigma, Acros, STREM, VWR or TCI and were used as received, without further purification. All glassware were oven or flame dried immediately prior to use. Tetrahydrofuran, acetonitrile, n-pentane, and diethyl ether were degassed and dried by passage through a series of drying columns using an MBRAUN SPS. All solvents were stored over 4 Å molecular sieves. Solvents were frequently tested using a standard solution of sodium benzophenone ketyl radical in THF to confirm the absence of trace amounts of water.

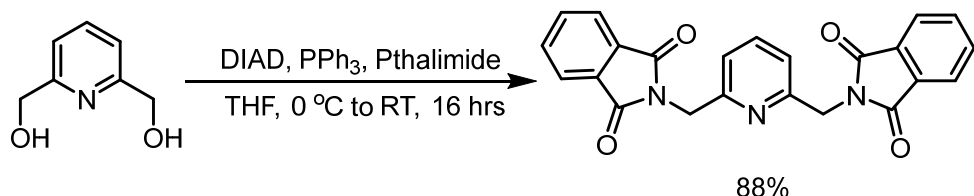
NMR spectra were recorded at ambient temperature unless otherwise stated on a Varian 500 MHz instrument. ^1H NMR chemical shifts are referenced to residual solvent and are reported in parts per million. Magnetic moments were calculated using the Evans method for a known concentration of the metal complex, with a sealed capillary containing the desired solvent.¹⁻² EPR spectra were recorded using a Bruker 10" EMXPlus X-band Continuous Wave EPR spectrometer at 77 K. Elemental analysis was carried out by the Microanalysis Laboratory at UIUC using an Exeter Analytical - Model CE440 CHN Analyzer. The geometry index was calculated based on published procedures and represented as tau (τ).³⁻⁴

Cyclic voltammetry (CV) was performed using a CHI-600D Electrochemical Analyzer. Electrochemical analysis was performed in a standard three-electrode cell using a glassy carbon disk (d=1.6 mm) working electrode, Pt wire counter electrode, and a non-aqueous Ag/AgNO₃ counter electrode. Experiments were conducted with 2.0 mM analyte and 0.1 M $^n\text{Bu}_4\text{NPF}_6$ (TBAP) as a supporting electrolyte in MeCN under a nitrogen atmosphere. All spectra and values are reported against ferrocene as an external standard.

II. Experimental Details

The ligands $^{Me}N_3CBr$ and $^{Me}N_3CH$ were synthesized according to a modified procedure based on previous publications.⁵⁻⁶

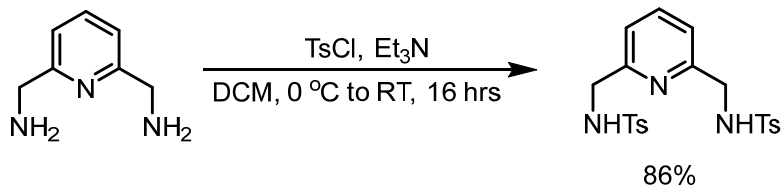
Synthesis of 2,6-bis(phthalimidomethyl)pyridine



Scheme S1. Synthesis of 2,6-bis(phthalimidomethyl)pyridine.

2,6-bis(phthalimidomethyl)pyridine was synthesized according to a modified literature procedure.⁷ To a 500-mL round-bottom flask charged with a stir bar, 2,6-bis(hydroxymethyl)pyridine (5.00 g, 35.9 mmol, 1.0 equiv) and triphenylphosphine (19.0 g, 72.4 mmol, 2.0 equiv) were dissolved in THF (300 mL) and cooled to 0 °C. Phthalimide (10.9 g, 74.4 mmol, 1.0 equiv) was added, after which diisopropyl azodicarboxylate ester (15.0 mL, 76.2 mmol, 1.0 equiv) was added dropwise. The mixture was allowed to warm to room temperature and stirred overnight. The crude mixture was filtered, and the solid was taken up in 8:1 DCM:THF (400 mL). The suspension was stirred for 30 minutes, after which the mixture was filtered. The solid was washed with DCM (2 × 25 mL) and dried to yield the product as a white-beige powder (12.4 g, 88%). Spectroscopic characterization matches previously reported values.

Synthesis of 2,6-bis(4-toluenesulfonylaminomethyl)pyridine

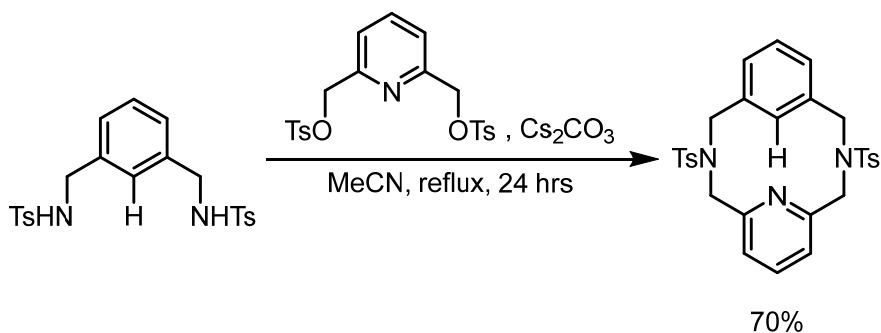


Scheme S2. Synthesis of tosyl-protected amine.

2,6-bis(4-toluenesulfonylaminomethyl)pyridine was synthesized according to a modified literature procedure.⁶ 2,6-bis(aminomethyl)pyridine (2.00 g, 14.6 mmol) and triethylamine (6.00 mL, 36.5 mmol, 2.5 equiv) were dissolved in DCM (100 mL) and cooled to 0 °C. A solution of 4-

toluenesulfonylchloride (8.34 g, 43.7 mmol, 1.5 equiv) in DCM (150 mL) was added dropwise, after which the mixture was allowed to warm to room temperature and stirred overnight. The mixture was washed with sat. NaHCO₃ solution (100 mL), dried over MgSO₄, and concentrated by rotary evaporation. The residue was recrystallized in hot ethanol to yield the product as off-white crystals (5.59 g, 86%). Spectroscopic characterization matches previously reported values.

Synthesis of 3,7-ditosyl-3,7-diaza-1(2,6)-pyridina-5(1,3)-benzenacyclooctaphane (^{Me}N3CH)



Scheme S3. Synthesis of ^{Me}N3CH.

2,6-bis(4-toluenesulfonylaminomethyl)benzene (3.8 g, 8.8 mmol, 1.0 equiv) and Cs₂CO₃ (7.00 g, 21.5 mmol, 2.5 equiv) were dissolved in MeCN (70 mL) and brought to reflux. Once refluxing, a solution of 2,6-bis(tosylmethyl)pyridine (3.94 g, 8.8 mmol, 1.0 equiv) in MeCN (100 mL) was added dropwise. Once addition was complete, the mixture was refluxed for an additional 24 hours. The solution was allowed to cool to room temperature and filtered. The solvent was removed from the filtrate by rotary evaporation, and the residue was recrystallized in chloroform/ethanol to yield the product as tan crystals (3.36 g, 70%). Spectroscopic characterization matches previously reported values.

Synthesis of ^{Me}N3CBr/^{Me}N3CH Nickel Complexes

All procedures were as previously reported, with slight modifications in some cases.^{8-10 11}

^{Me}N3CNi^{II}Br (1)

A solution of ^{Me}N3CBr (54.0 mg, 0.16 mmol, 1.0 equiv) in 2 mL of THF at -35 °C, was added Ni(COD)₂ (41 mg, 0.16 mmol, 1.0 equiv) and the reaction was stirred at room temperature for 6 hours. A filtration was applied to remove the residual black solid. The reaction was concentrated,

and cold pentane was added to crash out the product as a reddish solid. The product was washed with pentane (2×1 mL) and dried under vacuum. This product obtained as red powder was used without further purification due to its air sensitivity (yield: 43.6 mg, 69%). X-Ray quality crystals were grown by slow evaporation of pentane into a concentrated THF solution of the complex. Characterized properties are identical to reported values.⁸

$[\text{MeN}_3\text{CNi}^{\text{II}}(\text{MeCN})_2]\text{[PF}_6\text{]} \text{ (2)}$

To a solution of **1** (50 mg, 0.12 mmol, 1.0 equiv) in 1 mL of CH₃CN, TiPF₆ (42 mg, 0.12 mmol, 1.0 equiv) was added at RT. The reaction was stirred for 1 hour and the white TiBr precipitate was removed by filtration. The reaction was concentrated to 1 mL under vacuum. To this reaction, 3 mL of Et₂O was added and the product was crashed out as a brown solid. The product was washed with Et₂O (3×1 mL) and dried under vacuum. This product was used without further purification due to its air sensitivity and eluded more detailed characterization (yield: 54.8 mg, 81%).

HRMS (ESI+) calc. for C₁₉H₂₃N₄Ni⁺ [M–CH₃CN–PF₆]⁺: 365.1276; found: 365.1331; calc. for C₁₈H₂₀N₃Ni⁺ [M–2CH₃CN–PF₆]⁺: 324.1011; found: 324.1014.

UV-Vis (MeCN): λ_{max} (nm) (ϵ , M⁻¹ cm⁻¹): 267 (3878), 454 (331), 675 (102)

$[\text{MeN}_3\text{CNi}^{\text{III}}\text{Br}(\text{MeCN})]\text{[PF}_6\text{]} \text{ (3)}$

To a solution of **1** (35 mg, 0.09 mmol, 1.0 equiv) in 1.5 mL MeCN, FcPF₆ (27 mg, 0.09 mmol, 1.0 equiv) was added at RT. A green colored solution developed immediately and the reaction was stirred for additional one hour. The resulting solution filtered to remove any precipitate and the filtrate was concentrated and extracted with dry Et₂O. The final product obtained as a green powder was washed with Et₂O (5×1 mL) and dried under vacuum (yield: 43 mg, 84%). Attempt to obtain X-ray quality crystals was unsuccessful.

Elemental analysis for C₂₁H₂₈BrF₆N₄NiP [M•0.5Et₂O]: calc. C, 40.12; H, 4.46; N, 8.92. Found C, 40.02; H, 4.01; N, 9.06

HRMS (ESI+) calc. for C₁₇H₂₀N₃BrNi⁺ [M–CH₃CN–2PF₆]⁺: 403.0194, found: 403.0186; calc. for C₁₇H₂₀N₃Ni²⁺ [M–CH₃CN–Br–2PF₆]²⁺: 162.0505, found: 162.0510.

UV-Vis (MeCN): λ_{max} (nm) (ϵ , M⁻¹ cm⁻¹): 412 (782), 633 (255)

Evans' method (292 K, CD₃CN): $\mu_{\text{eff}} = 1.89 \pm 0.13 \mu_B$

^{Me}N₃CNi^{III}(Cl)₂ (4)

To a solution of **3** (62 mg, 0.1 mmol, 1.0 equiv) in 1 mL of CH₃CN, LiCl (45 mg, 1 mmol, 10 equiv) was added under ambient condition. 4 mL of MeOH was added to dissolve this mixture and the reaction was stirred for 2 hours. The resulting green solution was filtered and concentrated under vacuum. To this concentrated solution, 2 mL of DCM and 2 mL of brine was added. The aqueous phase was collected and extracted with DCM. This organic layer dried with MgSO₄ and concentrated to a green precipitate. This green precipitate was washed with Et₂O (3 × 1 mL) and dried under vacuum resulting to a green powder (yield: 24 mg, 58%). This green precipitate was dissolved in MeCN and layered with Et₂O to obtain dark green crystals of X-ray quality after 2 days at RT (yield: 21 mg, 70%) All properties are identical the reported values.⁸

[^{Me}N₃CNi^{III}(MeCN)₂][PF₆]₂ (5)

To a solution of **3** (25 mg, 0.04 mmol, 1.0 equiv) in 1.5 mL MeCN, AgPF₆ (11 mg, 0.04 mmol, 1.0 equiv) was added at RT. The reaction was stirred for an hour and the formed precipitates were removed by filtration, and the filtrate was layered with Et₂O. Dark green crystals of X-ray quality formed after 2 days at RT (yield: 21 mg, 70%). Alternatively, using the same procedure with 1 equiv TiPF₆, the same product was obtained in 66% yield. Also, with complex **1** and 2 equiv AgPF₆, 68% of product obtained.

Elemental analysis calculated for C₂₁H₂₆F₁₂N₅NiP₂: C, 36.18; H, 3.76; N, 10.05. Found: C, 35.90; H, 3.93; N, 10.41.

HRMS (ESI+) calc. for C₁₇H₂₀N₃Ni²⁺ [M–2CH₃CN–2PF₆]²⁺: 162.0505, found: 162.0505.

UV-Vis (MeCN): λ_{max} (nm) (ϵ , M⁻¹ cm⁻¹): 258 (4744), 307 (2334), 449 (165), 580 (112), 710 (74).

Evans method (CD₃CN, 292 K): 1.80 ± 0.18 μ B.

^{Me}N₃CHNi^{II}(Cl)₂/^{Me}N₃CHNi^{II}(Br)₂ (6a and 6b)

To a solution of ^{Me}N₃CH (10 mg, 0.075 mmol, 1 equiv) in 2 mL MeCN, NiCl₂[(CH₂OCH₃)₂] (16.5 mg, 0.075 mmol, 1 equiv) was added at RT. The reaction mixture was stirred at RT overnight, and the resulting green solution was layered with Et₂O at RT to yield light green crystals of X-ray quality after one day (yield: 13.6 mg, 67%).

Elemental analysis calculated for C₁₇H₂₁Cl₂N₃Ni: C, 51.44; H, 5.33; N, 10.59. Found: C, 50.98; H, 5.29; N, 10.17.

UV-Vis (MeCN): λ_{max} (nm) (ϵ , M⁻¹ cm⁻¹): 265 (5011), 344 (255), 431 (90), 711 (24)

Evans method (292 K, CD₃CN): 3.16 ± 0.24 μ B.

Using the same procedure, a solution of ^{Me}N₃CH (60 mg, 0.26 mmol, 1 equiv) in 2 mL THF was added to NiBr₂[(CH₂OCH₃)₂] (81 mg, 0.26 mmol, 1 equiv) to yield 72.4 mg (67%) of final product. Elemental analysis calculated for C₁₇H₂₁Br₂N₃Ni: C, 42.02; H, 4.36; N, 8.65. Found: C, 42.17; H, 4.43; N, 8.59.

UV-Vis (MeCN): λ_{max} (nm) (ϵ , M⁻¹ cm⁻¹): 267 (6861), 364 (640), 433 (73), 654 (46), 707 (40)

Evans method (295 K, CD₃CN): 3.12 ± 0.16 μ B.

[^{Me}N₃CHNi^{II}(MeCN)₂][PF₆]₂ (7)

To a solution of **6** (X=Br) (18.5 mg, 0.038 mmol, 1.0 equiv) in 2 mL MeCN, TiPF₆ (27 mg, 0.076 mmol, 1.0 equiv) was added at RT. The reaction mixture was stirred for an hour, and the resulting purple solution was layered with Et₂O at RT to yield purple crystals of X-ray quality after one day (yield: 22.5 mg, 85%).

Elemental analysis calculated for C₂₁H₂₇F₁₂N₅NiP₂: C, 36.13; H, 3.90; N, 10.03. Found: C, 36.18; H, 3.75; N, 10.63.

UV-Vis (MeCN): λ_{max} (nm) (ϵ , M⁻¹ cm⁻¹): 268 (5584), 373 (287), 557 (24).

Evans method (295 K, CD₃CN): 2.96 ± 0.18 μ B.

III. Reactivity Studies

Catalytic 2,2,2-trifluoroethoxylation (Scheme 3 from main text)

The catalytic ethoxylation of $^{Me}N_3CH$ was performed based on the procedure reported by Ribas et. al, with minor modifications.¹² For reactions using the nickel precursors, additional $^{Me}N_3CH$ was added to maintain the overall amount of substrate. Yields and conversions are reported with respect to a 1,3,5-trimethoxybenzene internal standard.

Table S1. Comparison of different Ni complexes and precursors.

Complex	Name	Mol %	Yield (%)	Conversion (%)
2	$[(^{Me}N_3C)Ni^{II}(MeCN)_2](PF_6)_2$	30	27	29
6b	$(^{Me}N_3CH)Ni^{II}Br_2$	30	25	31
6b	$(^{Me}N_3CH)Ni^{II}Br_2$	100	12	46
7	$[(^{Me}N_3CH)Ni^{II}(MeCN)_2](PF_6)_2$	20	27	29
7	$[(^{Me}N_3CH)Ni^{II}(MeCN)_2](PF_6)_2$	30	49	>99
NiBr₂(dme)	—	30	24	67
[Ni(MeCN)₂](BF₄)₂	—	30	29	53

C–C bond formation reactions (Scheme 4 from main text)

In a 4-mL vial charged with a stir bar under N₂ atmosphere, the Ni complex (5 μmol, 1.0 equiv) was dissolved in 2 mL THF. 2M octyl magnesium chloride in THF was added in one shot, and the reaction was stirred at room temperature. Under air, the reactions were quenched by either sat. NH₄Cl solution or conc. HCl and extracted with Et₂O (2 × 1 mL). The organic layers are combined, dried over MgSO₄, filtered through Celite, and analyzed by GC-FID using dodecane as an internal standard.

Table S2. Reaction conditions for reactivity with OctMgCl.

Entry	Complex	Equiv OctMgCl	Reaction Time	Workup
1 ^a	1	1.0	1 h	NH ₄ Cl
2 ^a	3	1.0	1 h	NH ₄ Cl
3 ^a	7 ^b	1.0	1 h	NH ₄ Cl
4	1	1.2	2 h	NH ₄ Cl
5	1	1.2	2 h	HCl
6	1	2.0	2 h	NH ₄ Cl
7	3	1.2	2 h	NH ₄ Cl
8	3	1.2	2 h	HCl
9	3	2.0	2 h	NH ₄ Cl
10	4 ^c	1.2	2 h	NH ₄ Cl

^a The organic layer was filtered through silica instead of Celite.

^b [(^{Me}N₃CH)Ni^{II}(MeCN)₂](PF₆)₂

^c (^{Me}N₃C)Ni^{III}Cl₂

Table S3. Detection of various products, as detected by GC-FID.

Entry	A (%)	B (%)	C (%)	D (%)	E (%)	A : E	A+C : E
1	2	<1	<1	18	41	0.053	0.053
2	7	<1	6	25	31	0.22	0.42
3	1	<1	9	24	29	0.038	0.34
4	9 ± 2	43 ± 2	<1	28 ± 5	37 ± 2	0.24 ± 0.06	0.24 ± 0.06
5	<1	1	<1	32	39	—	—
6	11	13	<1	41	49	0.22	0.22
7	33 ± 7	53 ± 13	3 ± 1	16 ± 7	21 ± 7	1.6 ± 0.6	1.7 ± 0.6
8	1	2	3	24	30	0.037	0.15
9	32	32	4	37	50	0.62	0.71
10	22	74	1	33	40	0.56	0.59

IV. UV-Vis Spectra

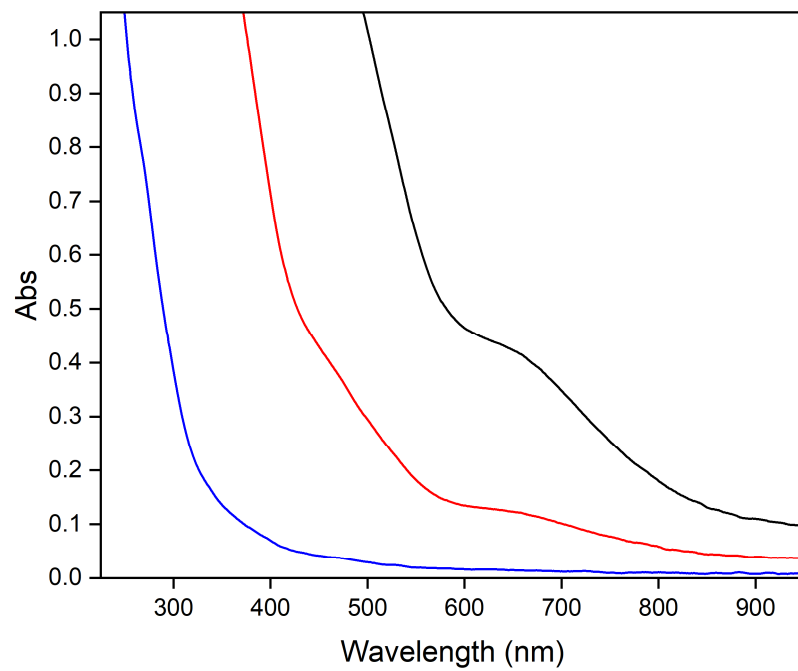


Figure S1. UV-Vis spectra of **2** collected at 4.0 mM (black), 1.5 mM (red), and 0.2 mM (blue)

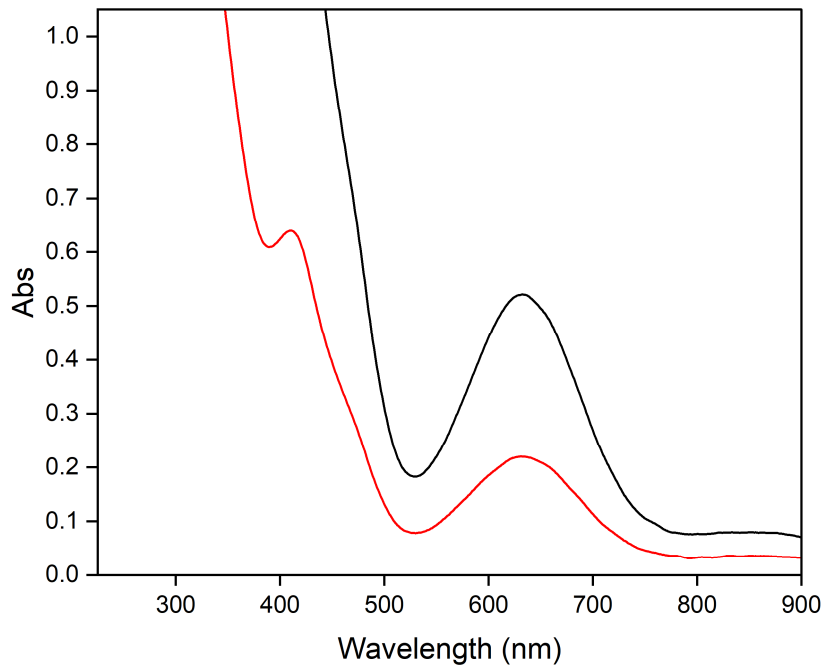


Figure S2. UV-Vis spectra of **3** collected at 2.0 mM (black) and 0.8 mM (red)

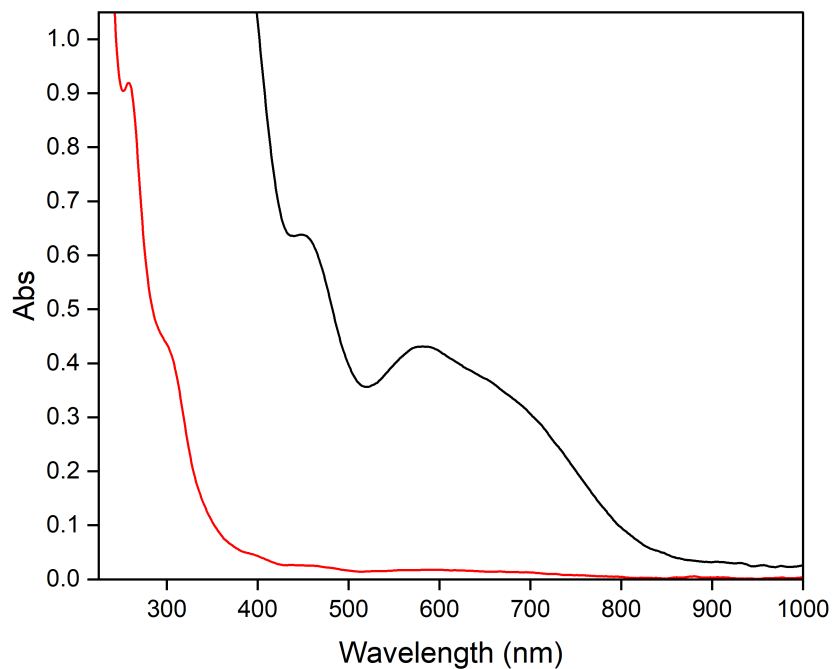


Figure S3. UV-Vis spectra of **5** collected at 4.0 mM (black) and 0.2 mM (red)

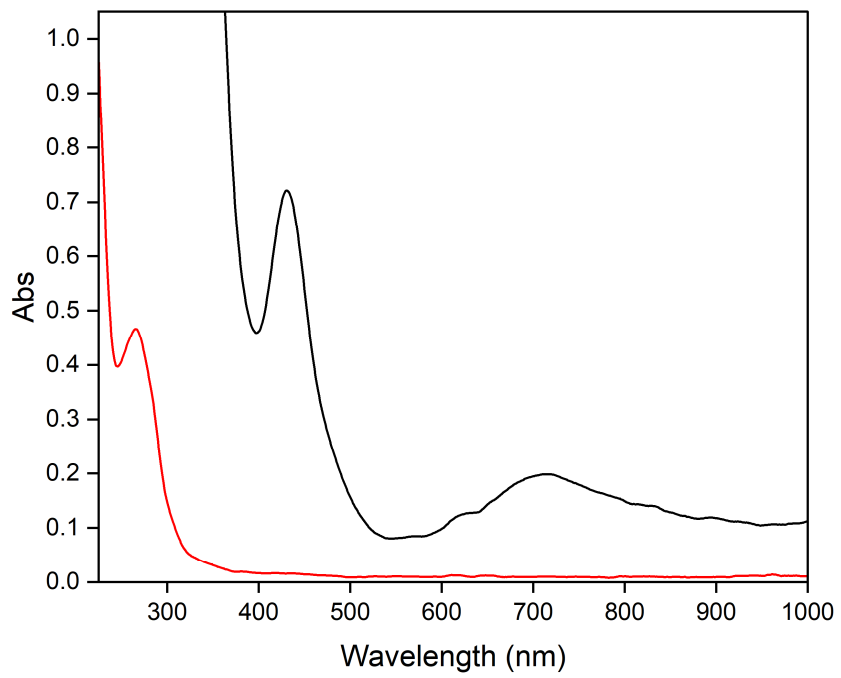


Figure S4. UV-Vis spectra of **6a** collected at 8.0 mM (black) and 0.1 mM (red)

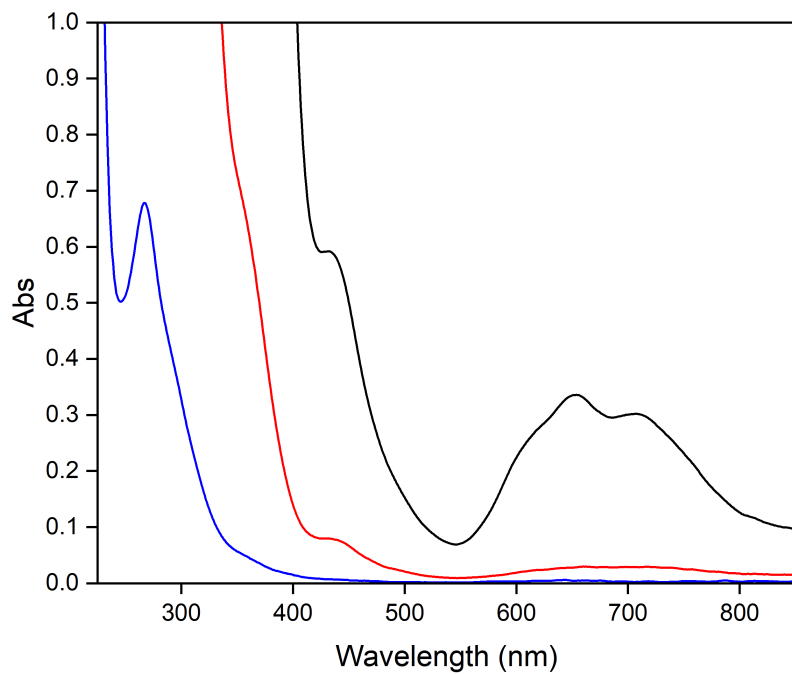


Figure S5. UV-Vis spectra of **6b** collected at 8.0 mM (black), 1.0 mM (red), and 0.1 mM (blue)

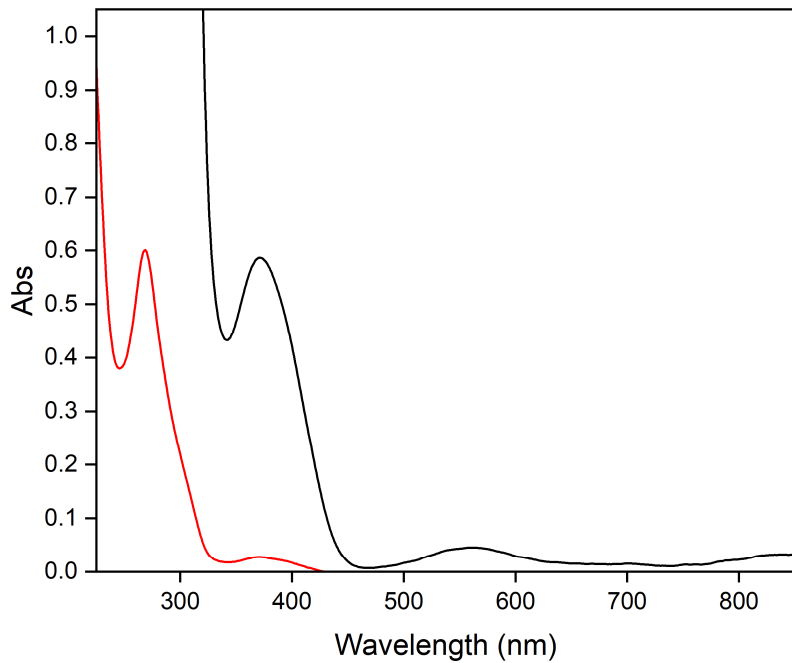


Figure S6. UV-Vis Spectra of **7** collected at 2.0 mM (black) and 0.1 mM (red)

V. Cyclic Voltammograms

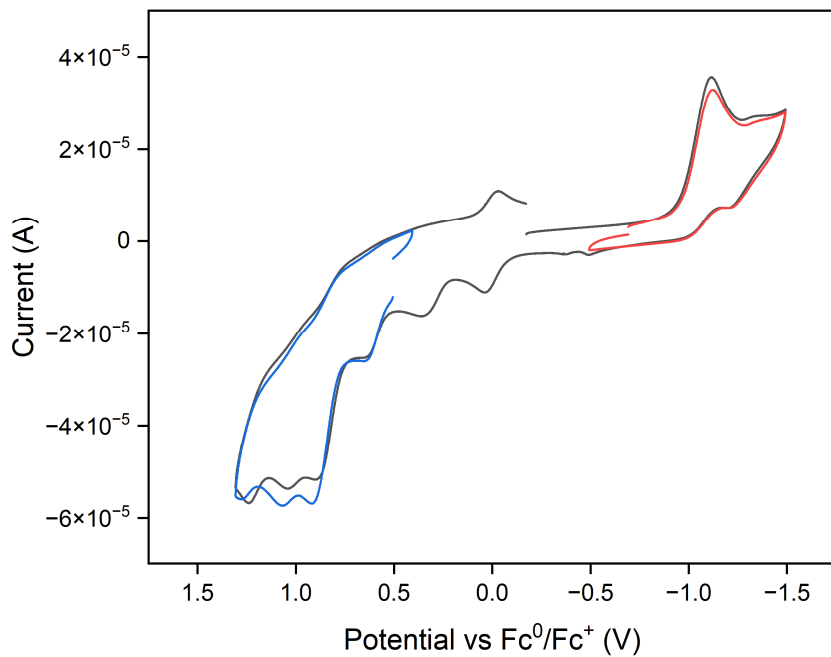


Figure S7. Cyclic voltammogram of **3**, recorded at 100 mV/s.

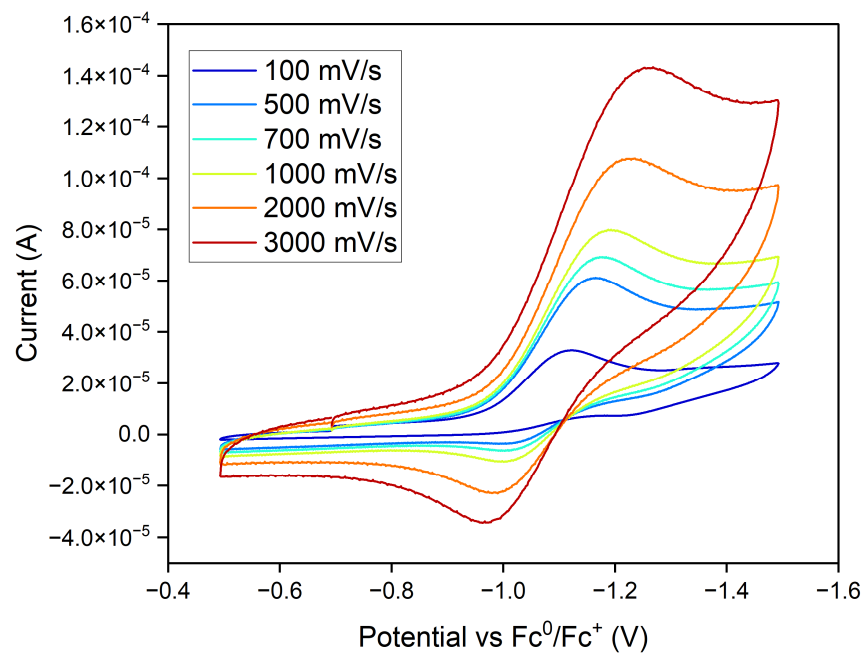


Figure S8. Cyclic voltammogram of reduction event at -1.2 V for **3**. Growth of a reverse wave at higher scans indicates quasi-reversibility.

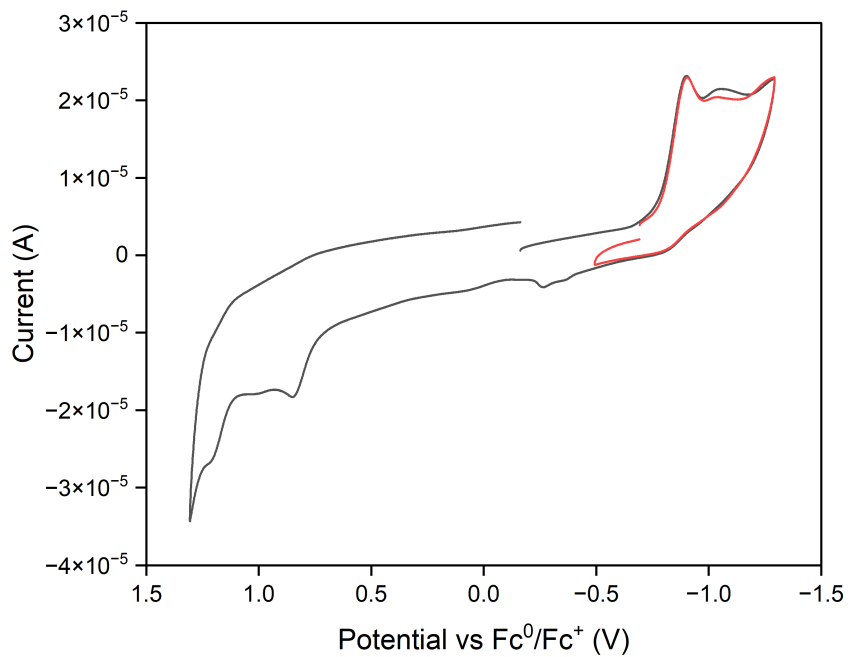


Figure S9. Cyclic voltammogram of **5**, recorded at 100 mV/s.

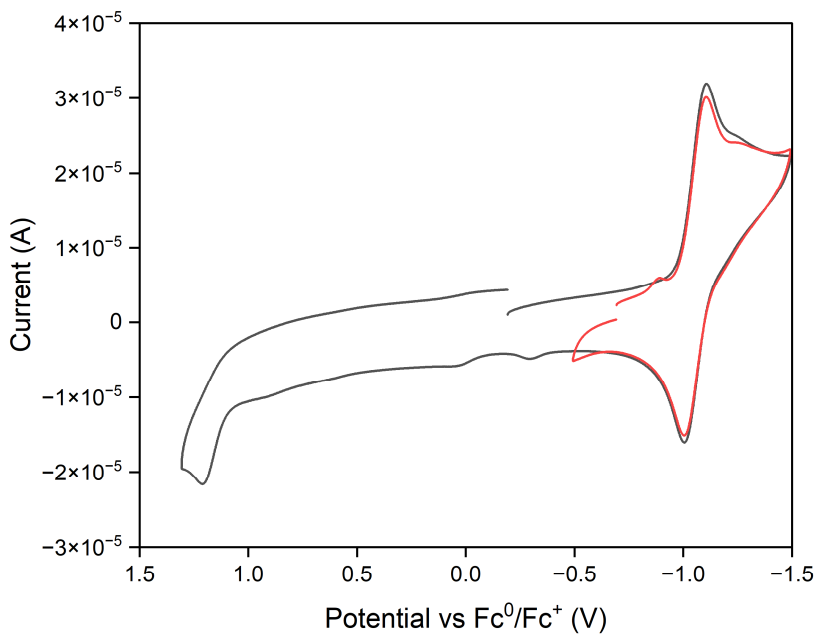


Figure S10. Cyclic voltammogram of **7**, recorded at 100 mV/s.

VI. Computational Details

The molecular structures were optimized using B3LYP¹³⁻¹⁴ density functional combined with def2-TZVPP¹⁵⁻¹⁶ basis set. The nature of local minima was confirmed by checking the Hessian matrix of energy. All DFT computations were performed by Gaussian 16 Rev. C1 suite of programs.¹⁷ The Natural Bond Orbital (NBO) analysis results for complex **6b** is shown below.

Table S4. NBO analysis of **6b**, for both the alpha and beta spins; the average energies are reported in the main text.

Spin State	Donor	Atomic orbital	Type	q _i	Acceptor	Atomic orbital	Type	q _i	E(2) kcal/mol	E(j)-E(i) a.u	F(i,j)
α	C17—H37	C17 sp ^{2.5} H37 s	σ	0.98537	Ni44	s(99.48%) p0.00(0.24%) d 0.00(0.29%) f 0.00(0.00%)	LV	0.17552	2.08	0.53	0.042
	Br40	s(0.02%) p 99.99 (99.95%) d 0.00(0.03%)	LP	0.98407	C17—H37	C 17 sp ^{2.5} H 37 s	σ*	0.02354	2.62	0.67	0.053
Spin State	Donor	Atomic orbital	Type	Q _i	Acceptor	Atomic orbital	Type	q _i	E(2) kcal/mol	E(j)-E(i) a.u	F(i,j)
β	C17—H37	C17 sp ^{2.47} H37 s	σ	0.97110	Ni44	s(17.09%) p 0.02(0.24%) d 4.83(82.62%) f 0.00(0.00%)	LV	0.11397	2.43	0.52	0.045
	Br40	s(7.18%) p12.92 (92.79%) d 0.00(0.03%)	LP	0.97675	C17—H37	C 17 sp ^{2.47} H 37 s	σ*	0.02368	3.58	0.70	0.70

Coordinates of optimized structure **6b**

Charge= 0; Multiplicity= 3;
 Br -0.947161 0.336282 12.28504
 Ni 0.125606 2.411249 11.527005
 N 0.656376 4.323539 11.010112
 N 0.550963 3.406129 13.615631
 N -1.058752 2.74484 9.525839
 C 0.435362 4.743217 9.765481
 C 1.276514 5.089897 11.90579
 C -2.474526 4.219453 10.941251
 C -1.116944 1.500718 8.734683
 C -1.595817 4.579508 13.176143
 C -0.70685 3.952325 14.222264
 C 1.516976 4.463842 13.260239
 C -2.448971 3.23907 9.793927

C 1.171381 2.439161 14.541295
C -2.043871 3.734762 12.169187
C -0.221125 3.746797 8.838141
C 1.742079 6.351673 11.559425
C 0.873672 5.993556 9.34938
C -1.828128 5.945825 13.043657
C 1.541403 6.800331 10.260945
C -2.433693 6.435814 11.88738
C -2.704228 5.586836 10.81512
Br 2.337232 1.636698 10.782492
H -0.106 1.127373 8.58785
H -1.593878 1.662436 7.759827
H -1.672852 0.753002 9.294476
H -1.216447 3.104582 14.678373
H -0.457256 4.664153 15.018184
H 2.500813 3.992664 13.209908
H 1.566402 5.240643 14.032885
H -2.870524 3.676473 8.881026
H -3.039499 2.359735 10.047753
H 0.469825 1.630034 14.727389
H 1.452353 2.910469 15.491515
H 2.055111 2.015344 14.069728
H -1.960327 2.65985 12.309724
H -0.781204 4.270652 8.054109
H 0.589815 3.202093 8.350097
H 2.247046 6.967212 12.290883
H 0.693362 6.326333 8.336632
H -1.510961 6.632729 13.818666
H 1.894982 7.778534 9.963496
H -2.627155 7.496142 11.792604
H -3.060104 5.998023 9.878445

VII. X-ray Structure Determinations

General information.

Crystallographic data for the structures reported in this article have been deposited at the Cambridge Crystallographic Data Centre, under CCDC deposition numbers 2390120, 2390122-2390125. Crystals were mounted on a Bruker D8 Venture kappa diffractometer equipped with a Photon II CPAD detector. An I μ s microfocus Mo source ($\lambda = 0.71073 \text{ \AA}$) coupled with a multi-layer mirror monochromator provided the incident beam. The sample was mounted on a nylon loop with the minimal amount of Paratone-N oil. Data was collected as a series of ϕ and/or ω scans at 100 K using a cold stream of N₂(g). The collection, cell refinement, and integration of intensity data was carried out with the APEXIII software.¹⁸ A multiscan absorption correction was performed with SADABS or TWINABS-2012/1.¹⁸ The structure was phased with intrinsic methods using SHELXT and refined with the full-matrix least squares program SHELXL.¹⁹ Hydrogen atoms were placed in calculated positions using the standard riding model and refined isotropically; all non-hydrogen atoms were refined anisotropically. Software and solutions: SAINT V8.38A, SHELXT, XL, Olex2.¹⁹⁻²¹

X-ray structure determination of [(^{Me}N₃C)Ni^{II}Br (1)

Table S5. Crystal data and structure refinement for **1**.

Identification code	1
Empirical formula	C ₁₇ H ₂₀ BrN ₃ Ni
Formula weight	404.98
Temperature/K	100.00
Crystal system	tetragonal
Space group	P4 ₃
a/Å	9.3768(8)
b/Å	9.3768(8)
c/Å	18.877(2)
α/°	90
β/°	90
γ/°	90
Volume/Å ³	1659.8(3)
Z	4
ρ _{calcd} /cm ³	1.621
μ/mm ⁻¹	3.576
F(000)	824.0
Crystal size/mm ³	0.317 × 0.14 × 0.034
Radiation	MoKα ($\lambda = 0.71073$)
2Θ range for data collection/°	4.344 to 50.656
Index ranges	-11 ≤ h ≤ 11, -9 ≤ k ≤ 11, -22 ≤ l ≤ 22
Reflections collected	13329
Independent reflections	3016 [R _{int} = 0.0707, R _{sigma} = 0.0614]
Data/restraints/parameters	3016/1/201
Goodness-of-fit on F ²	1.068
Final R indexes [I>=2σ (I)]	R ₁ = 0.0464, wR ₂ = 0.1003
Final R indexes [all data]	R ₁ = 0.0552, wR ₂ = 0.1034
Largest diff. peak/hole / e Å ⁻³	0.54/-0.49
Flack parameter	0.007(15)

Table S6. Bond Lengths for 1.

Atom	Atom	Length/Å	Atom	Atom	Length/Å
Br1	Ni1	2.3724(15)	C2	C4	1.392(14)
Ni1	N2	1.981(8)	C8	C7	1.523(13)
Ni1	N1	2.292(7)	C8	N3	1.502(13)
Ni1	C1	1.954(9)	C7	C1	1.382(12)
Ni1	N3	2.276(7)	C7	C6	1.361(14)
C3	C2	1.520(13)	C9	C10	1.499(13)
C3	N1	1.489(12)	C9	C11	1.391(14)
N2	C9	1.353(12)	N1	C16	1.461(12)
N2	C14	1.338(12)	N1	C10	1.461(13)
C15	N3	1.488(13)	C5	C4	1.388(13)
C15	C14	1.507(14)	C5	C6	1.373(14)
C13	C14	1.383(14)	N3	C17	1.493(12)
C13	C12	1.378(16)	C11	C12	1.379(15)
C2	C1	1.381(13)			

Table S7. Bond Angles for 1.

Atom	Atom	Atom	Angle/ [°]	Atom	Atom	Atom	Angle/ [°]
N2	Ni1	Br1	133.1(2)	C11	C9	C10	124.5(9)
N2	Ni1	N1	80.2(3)	C3	N1	Ni1	105.0(5)
N2	Ni1	N3	80.6(3)	C16	N1	Ni1	117.4(6)
N1	Ni1	Br1	101.5(2)	C16	N1	C3	110.4(7)
C1	Ni1	Br1	140.3(3)	C10	N1	Ni1	102.7(5)
C1	Ni1	N2	86.6(3)	C10	N1	C3	111.3(8)
C1	Ni1	N1	81.8(3)	C10	N1	C16	109.7(8)
C1	Ni1	N3	81.2(3)	C6	C5	C4	119.8(10)
N3	Ni1	Br1	103.4(2)	C2	C1	Ni1	117.6(7)
N3	Ni1	N1	154.9(3)	C2	C1	C7	118.6(9)
N1	C3	C2	112.8(7)	C7	C1	Ni1	118.5(6)
C9	N2	Ni1	117.4(6)	C15	N3	Ni1	105.0(6)
C14	N2	Ni1	118.2(7)	C15	N3	C8	111.8(8)
C14	N2	C9	120.1(8)	C15	N3	C17	108.2(7)
N3	C15	C14	112.6(7)	C8	N3	Ni1	103.3(5)
C12	C13	C14	118.6(10)	C17	N3	Ni1	118.8(6)
C1	C2	C3	116.1(8)	C17	N3	C8	109.6(8)
C1	C2	C4	120.8(9)	C5	C4	C2	119.0(9)
C4	C2	C3	123.1(8)	N1	C10	C9	111.8(8)
N3	C8	C7	110.7(7)	C12	C11	C9	118.9(10)
C1	C7	C8	114.0(8)	C7	C6	C5	120.8(9)
C6	C7	C8	125.1(8)	N2	C14	C15	115.7(9)
C6	C7	C1	120.8(8)	N2	C14	C13	121.7(9)
N2	C9	C10	115.0(8)	C13	C14	C15	122.5(9)
N2	C9	C11	120.5(9)	C13	C12	C11	120.1(10)

X-ray structure determination of $[({}^{\text{Me}}\text{N}_3\text{C})\text{Ni}^{\text{III}}(\text{MeCN})_2](\text{PF}_6)_2$ (5**)**

Table S8. Crystal data and structural refinement for **5**.

Identification code	mo_ed01t_0m
Empirical formula	C ₂₃ H ₂₉ F ₁₂ N ₆ NiP ₂
Formula weight	738.17
Temperature/K	100.00
Crystal system	monoclinic
Space group	P2 ₁ /c
a/Å	10.2675(3)
b/Å	18.8199(5)
c/Å	15.6377(4)
$\alpha/^\circ$	90
$\beta/^\circ$	97.2359(8)
$\gamma/^\circ$	90
Volume/Å ³	2997.66(14)
Z	4
$\rho_{\text{calc}}/\text{g/cm}^3$	1.636
μ/mm^{-1}	0.855
F(000)	1500.0
Crystal size/mm ³	0.572 × 0.152 × 0.044
Radiation	MoKα ($\lambda = 0.71073$)
2Θ range for data collection/°	3.998 to 52.818
Index ranges	-12 ≤ h ≤ 12, -23 ≤ k ≤ 23, -19 ≤ l ≤ 19
Reflections collected	72080
Independent reflections	6147 [R _{int} = 0.0337, R _{sigma} = 0.0157]
Data/restraints/parameters	6147/0/402
Goodness-of-fit on F ²	1.045
Final R indexes [I>=2σ (I)]	R ₁ = 0.0353, wR ₂ = 0.0855
Final R indexes [all data]	R ₁ = 0.0383, wR ₂ = 0.0872
Largest diff. peak/hole / e Å ⁻³	0.63/-0.51

Table S9. Bond lengths for **5**.

Atom	Atom	Length/Å	Atom	Atom	Length/Å
Ni1	N1	1.9351(18)	N3	C7	1.501(3)
Ni1	N2	2.1519(18)	N3	C8	1.492(3)
Ni1	N3	2.1417(18)	N3	C17	1.486(3)
Ni1	N4	1.9825(18)	N4	C18	1.133(3)
Ni1	N5	1.9899(18)	N5	C20	1.139(3)
Ni1	C1	1.921(2)	N6	C22	1.136(4)
P1	F1	1.6017(14)	C1	C2	1.365(3)
P1	F2	1.5973(15)	C1	C6	1.359(3)
P1	F3	1.6031(14)	C2	C3	1.392(4)
P1	F4	1.6005(15)	C2	C15	1.496(4)
P1	F5	1.5949(14)	C3	C4	1.393(4)
P1	F6	1.5971(14)	C4	C5	1.386(4)
P2	F7	1.5859(18)	C5	C6	1.392(3)
P2	F8	1.5990(15)	C6	C7	1.493(3)
P2	F9	1.574(2)	C8	C9	1.502(3)
P2	F10	1.5861(17)	C9	C10	1.382(3)
P2	F11	1.578(2)	C10	C11	1.386(4)
P2	F12	1.6030(18)	C11	C12	1.389(3)
N1	C9	1.345(3)	C12	C13	1.389(3)
N1	C13	1.346(3)	C13	C14	1.502(3)
N2	C14	1.491(3)	C18	C19	1.457(3)
N2	C15	1.493(3)	C20	C21	1.451(3)
N2	C16	1.486(3)	C22	C23	1.440(4)

Table S10. Bond angles for **5**.

Atom	Atom	Atom	Angle/ [°]	Atom	Atom	Atom	Angle/ [°]
N1	Ni1	N2	82.38(7)	C9	N1	Ni1	118.04(15)
N1	Ni1	N3	82.10(7)	C9	N1	C13	122.89(19)
N1	Ni1	N4	176.36(8)	C13	N1	Ni1	119.01(15)
N1	Ni1	N5	91.99(8)	C14	N2	Ni1	107.54(13)
N3	Ni1	N2	159.40(7)	C14	N2	C15	111.4(2)
N4	Ni1	N2	97.51(7)	C15	N2	Ni1	105.46(14)
N4	Ni1	N3	97.12(7)	C16	N2	Ni1	113.72(15)
N4	Ni1	N5	91.63(7)	C16	N2	C14	109.2(2)
N5	Ni1	N2	98.42(7)	C16	N2	C15	109.42(18)
N5	Ni1	N3	95.58(7)	C7	N3	Ni1	108.58(13)
C1	Ni1	N1	85.46(8)	C8	N3	Ni1	104.81(13)
C1	Ni1	N2	82.59(9)	C8	N3	C7	111.46(16)
C1	Ni1	N3	82.75(8)	C17	N3	Ni1	114.63(13)
C1	Ni1	N4	90.92(8)	C17	N3	C7	108.94(17)
C1	Ni1	N5	177.11(8)	C17	N3	C8	108.40(17)
F1	P1	F3	179.29(9)	C18	N4	Ni1	174.38(18)
F2	P1	F1	90.43(8)	C20	N5	Ni1	175.46(18)
F2	P1	F3	90.13(9)	C2	C1	Ni1	116.49(17)
F2	P1	F4	179.49(10)	C6	C1	Ni1	117.75(16)
F4	P1	F1	90.08(8)	C6	C1	C2	125.7(2)
F4	P1	F3	89.36(8)	C1	C2	C3	116.6(2)
F5	P1	F1	90.86(8)	C1	C2	C15	116.8(2)
F5	P1	F2	89.89(9)	C3	C2	C15	126.3(2)
F5	P1	F3	89.58(8)	C2	C3	C4	119.9(2)
F5	P1	F4	90.16(8)	C5	C4	C3	121.0(2)
F5	P1	F6	179.85(10)	C4	C5	C6	119.4(3)
F6	P1	F1	89.20(8)	C1	C6	C5	117.4(2)
F6	P1	F2	89.97(9)	C1	C6	C7	117.81(19)
F6	P1	F3	90.36(8)	C5	C6	C7	124.5(2)
F6	P1	F4	89.98(9)	C6	C7	N3	110.76(18)
F7	P2	F8	89.82(10)	N3	C8	C9	111.32(17)
F7	P2	F10	89.98(11)	N1	C9	C8	114.62(18)
F7	P2	F12	87.68(11)	N1	C9	C10	119.8(2)
F8	P2	F12	90.19(9)	C10	C9	C8	125.4(2)
F9	P2	F7	176.27(15)	C9	C10	C11	118.7(2)

Atom	Atom	Atom	Angle/[°]	Atom	Atom	Atom	Angle/[°]
F9	P2	F8	88.63(11)	C10	C11	C12	120.6(2)
F9	P2	F10	91.52(12)	C11	C12	C13	118.8(2)
F9	P2	F11	93.02(16)	N1	C13	C12	119.2(2)
F9	P2	F12	88.93(13)	N1	C13	C14	115.7(2)
F10	P2	F8	179.06(11)	C12	C13	C14	124.9(2)
F10	P2	F12	88.89(10)	N2	C14	C13	112.8(2)
F11	P2	F7	90.33(14)	N2	C15	C2	109.68(18)
F11	P2	F8	88.59(10)	N4	C18	C19	178.7(2)
F11	P2	F10	92.33(11)	N5	C20	C21	179.2(2)
F11	P2	F12	177.67(13)	N6	C22	C23	178.4(5)

X-ray structure determination of (^{Me}N₃CH)Ni^{II}Cl₂ (6a)

Table S11. Crystal data and structural refinement for **6a**.

Identification code	mo_ed45x
Empirical formula	C ₁₉ H ₂₄ Cl ₂ N ₄ Ni
Formula weight	438.03
Temperature/K	100.00
Crystal system	orthorhombic
Space group	Pca2 ₁
a/Å	15.6090(4)
b/Å	8.7670(2)
c/Å	14.6494(3)
α/°	90
β/°	90
γ/°	90
Volume/Å ³	2004.68(8)
Z	4
ρ _{calc} g/cm ³	1.451
μ/mm ⁻¹	1.245
F(000)	912.0
Crystal size/mm ³	0.838 × 0.42 × 0.368
Radiation	MoKα ($\lambda = 0.71073$)
2Θ range for data collection/°	4.646 to 56.622
Index ranges	-20 ≤ h ≤ 20, -11 ≤ k ≤ 11, -19 ≤ l ≤ 19
Reflections collected	33927
Independent reflections	4996 [R _{int} = 0.0254, R _{sigma} = 0.0159]
Data/restraints/parameters	4996/1/250
Goodness-of-fit on F ²	1.072
Final R indexes [I>=2σ (I)]	R ₁ = 0.0188, wR ₂ = 0.0475
Final R indexes [all data]	R ₁ = 0.0191, wR ₂ = 0.0477
Largest diff. peak/hole / e Å ⁻³	0.27/-0.26
Flack parameter	0.007(5)

Table S12. Bond lengths for **6a**.

Atom	Atom	Length/Å	Atom	Atom	Length/Å
Ni1	Cl2	2.3288(5)	C6	C7	1.502(3)
Ni1	Cl1	2.3115(6)	C1	C2	1.390(3)
Ni1	N1	1.9926(17)	C9	C8	1.511(3)
Ni1	N2	2.2329(17)	C9	C10	1.387(3)
Ni1	N3	2.2418(16)	C14	C13	1.504(3)
N1	C9	1.336(3)	C5	C4	1.392(3)
N1	C13	1.343(3)	C13	C12	1.390(3)
N2	C16	1.477(3)	C4	C3	1.394(3)
N2	C14	1.485(2)	C12	C11	1.388(3)
N2	C15	1.509(3)	C11	C10	1.394(3)
N3	C8	1.484(3)	C2	C3	1.391(3)
N3	C17	1.481(3)	C2	C15	1.511(3)
N3	C7	1.510(3)	N4	C19	1.136(3)
C6	C1	1.395(3)	C18	C19	1.463(3)
C6	C5	1.393(3)			

Table S13. Bond angles for **6a**.

Atom	Atom	Atom	Angle/ [°]	Atom	Atom	Atom	Angle/ [°]
C11	Ni1	Cl2	97.16(2)	C1	C6	C7	115.52(19)
N1	Ni1	Cl2	91.33(5)	C5	C6	C1	118.6(2)
N1	Ni1	Cl1	171.51(5)	C5	C6	C7	124.4(2)
N1	Ni1	N2	79.30(6)	C2	C1	C6	121.4(2)
N1	Ni1	N3	79.98(7)	N1	C9	C8	115.18(18)
N2	Ni1	Cl2	102.49(5)	N1	C9	C10	121.05(19)
N2	Ni1	Cl1	98.96(5)	C10	C9	C8	123.69(18)
N2	Ni1	N3	147.74(6)	N2	C14	C13	112.19(16)
N3	Ni1	Cl2	102.46(4)	C4	C5	C6	120.0(2)
N3	Ni1	Cl1	97.89(5)	N1	C13	C14	114.35(17)
C9	N1	Ni1	119.41(14)	N1	C13	C12	120.79(19)
C9	N1	C13	121.37(17)	C12	C13	C14	124.77(18)
C13	N1	Ni1	119.16(14)	N3	C8	C9	113.28(16)
C16	N2	Ni1	113.30(13)	C5	C4	C3	120.2(2)
C16	N2	C14	109.11(17)	C11	C12	C13	118.23(19)
C16	N2	C15	108.83(16)	C12	C11	C10	120.38(19)
C14	N2	Ni1	103.68(12)	C9	C10	C11	118.15(19)
C14	N2	C15	110.81(17)	C1	C2	C3	118.7(2)
C15	N2	Ni1	111.02(13)	C1	C2	C15	115.34(19)
C8	N3	Ni1	104.54(12)	C3	C2	C15	124.8(2)
C8	N3	C7	110.49(17)	C2	C3	C4	120.0(2)
C17	N3	Ni1	113.05(13)	N2	C15	C2	108.84(16)
C17	N3	C8	109.37(17)	C6	C7	N3	107.36(16)
C17	N3	C7	108.69(17)	N4	C19	C18	178.6(3)
C7	N3	Ni1	110.65(12)				

X-ray structure determination of (^{Me}N₃CH)Ni^{II}Br₂ (6b)

Table S14. Crystal data and structural refinement for **6b**.

Identification code	mo_ED53W_0m
Empirical formula	C ₁₇ H ₂₁ Br ₂ N ₃ Ni
Formula weight	485.90
Temperature/K	100.00
Crystal system	orthorhombic
Space group	Pbca
a/Å	12.8864(3)
b/Å	15.0143(3)
c/Å	18.1804(4)
α/°	90
β/°	90
γ/°	90
Volume/Å ³	3517.55(13)
Z	8
ρ _{calc} g/cm ³	1.835
μ/mm ⁻¹	5.649
F(000)	1936.0
Crystal size/mm ³	0.318 × 0.27 × 0.142
Radiation	MoKα ($\lambda = 0.71073$)
2Θ range for data collection/°	4.48 to 56.67
Index ranges	-17 ≤ h ≤ 17, -20 ≤ k ≤ 20, -24 ≤ l ≤ 24
Reflections collected	97734
Independent reflections	4382 [R _{int} = 0.0446, R _{sigma} = 0.0135]
Data/restraints/parameters	4382/0/215
Goodness-of-fit on F ²	1.028
Final R indexes [I>=2σ (I)]	R ₁ = 0.0172, wR ₂ = 0.0408
Final R indexes [all data]	R ₁ = 0.0201, wR ₂ = 0.0420
Largest diff. peak/hole / e Å ⁻³	0.54/-0.32

Table S15. Bond lengths for **6b**.

Atom	Atom	Length/ \AA	Atom	Atom	Length/ \AA
Br1	Ni1	2.4546(2)	C17	C6	1.511(2)
Ni1	N3	1.9850(13)	C17	C16	1.385(2)
Ni1	N1	2.2232(13)	C13	C4	1.506(2)
Ni1	N2	2.2548(13)	C13	C14	1.389(2)
Ni1	C8	2.4819(15)	C7	C5	1.505(2)
Ni1	Br2	2.4782(2)	C7	C8	1.390(2)
N3	C17	1.3397(19)	C7	C12	1.397(2)
N3	C13	1.3403(19)	C9	C3	1.507(2)
N1	C3	1.5078(19)	C9	C8	1.389(2)
N1	C4	1.4912(19)	C9	C10	1.394(2)
N1	C2	1.4819(19)	C14	C15	1.388(2)
N2	C1	1.4825(19)	C16	C15	1.393(2)
N2	C5	1.5068(19)	C10	C11	1.395(2)
N2	C6	1.4880(19)	C11	C12	1.397(2)

Table S16. Bond angles for **6b**.

Atom	Atom	Atom	Angle/ [°]	Atom	Atom	Atom	Angle/ [°]
Br1	Ni1	C8	91.86(4)	C6	N2	Ni1	104.30(9)
Br1	Ni1	Br2	97.680(8)	C6	N2	C5	110.70(12)
N3	Ni1	Br1	173.61(4)	N3	C17	C6	115.13(13)
N3	Ni1	N1	80.10(5)	N3	C17	C16	120.84(14)
N3	Ni1	N2	79.64(5)	C16	C17	C6	123.87(14)
N3	Ni1	C8	81.90(5)	N3	C13	C4	114.90(13)
N3	Ni1	Br2	88.65(4)	N3	C13	C14	120.87(14)
N1	Ni1	Br1	99.87(3)	C14	C13	C4	124.04(13)
N1	Ni1	N2	148.65(5)	C8	C7	C5	115.37(14)
N1	Ni1	C8	76.68(5)	C8	C7	C12	118.43(14)
N1	Ni1	Br2	97.29(3)	C12	C7	C5	125.16(14)
N2	Ni1	Br1	97.68(3)	C8	C9	C3	115.06(14)
N2	Ni1	C8	76.98(5)	C8	C9	C10	119.10(14)
N2	Ni1	Br2	105.87(3)	C10	C9	C3	125.10(14)
Br2	Ni1	C8	169.52(4)	C9	C3	N1	108.67(12)
C17	N3	Ni1	119.93(10)	N1	C4	C13	112.81(12)
C17	N3	C13	121.32(13)	C7	C5	N2	109.08(12)
C13	N3	Ni1	118.69(10)	C7	C8	Ni1	101.48(10)
C3	N1	Ni1	111.52(9)	C9	C8	Ni1	101.06(9)
C4	N1	Ni1	103.49(9)	C9	C8	C7	121.75(15)
C4	N1	C3	110.06(12)	N2	C6	C17	113.55(12)
C2	N1	Ni1	113.36(9)	C15	C14	C13	118.34(14)
C2	N1	C3	108.93(12)	C17	C16	C15	118.47(14)
C2	N1	C4	109.35(12)	C9	C10	C11	118.97(15)
C1	N2	Ni1	115.38(10)	C14	C15	C16	120.16(14)
C1	N2	C5	107.86(12)	C10	C11	C12	121.23(15)
C1	N2	C6	109.12(12)	C7	C12	C11	119.37(15)
C5	N2	Ni1	109.46(9)				

X-ray structure determination of $[({}^{\text{Me}}\text{N}_3\text{CH})\text{Ni}^{\text{II}}(\text{MeCN})_2](\text{PF}_6)_2$ (7)

Table S17. Crystal data and structural refinement for 7.

Identification code	mo_ed36x_0m
Empirical formula	C ₂₃ H ₃₀ F ₁₂ N ₆ NiP ₂
Formula weight	739.18
Temperature/K	100.00
Crystal system	triclinic
Space group	P-1
a/Å	13.2054(4)
b/Å	13.5806(4)
c/Å	17.2734(5)
$\alpha/^\circ$	88.4600(10)
$\beta/^\circ$	89.9270(10)
$\gamma/^\circ$	80.0500(10)
Volume/Å ³	3050.05(16)
Z	4
$\rho_{\text{calc}}/\text{g/cm}^3$	1.610
μ/mm^{-1}	0.840
F(000)	1504.0
Crystal size/mm ³	0.561 × 0.311 × 0.26
Radiation	MoKα ($\lambda = 0.71073$)
2Θ range for data collection/°	3.802 to 52.868
Index ranges	-16 ≤ h ≤ 16, -16 ≤ k ≤ 17, -21 ≤ l ≤ 21
Reflections collected	168081
Independent reflections	12529 [$R_{\text{int}} = 0.0372$, $R_{\text{sigma}} = 0.0147$]
Data/restraints/parameters	12529/0/803
Goodness-of-fit on F ²	1.034
Final R indexes [I>=2σ (I)]	$R_1 = 0.0461$, $wR_2 = 0.1098$
Final R indexes [all data]	$R_1 = 0.0490$, $wR_2 = 0.1122$
Largest diff. peak/hole / e Å ⁻³	1.55/-1.34

Table S18. Bond lengths for 7.

Atom	Atom	Length/ \AA	Atom	Atom	Length/ \AA
Ni1	N1	1.971(2)	N10	C39	1.137(3)
Ni1	N2	2.179(2)	N8	C29	1.494(3)
Ni1	N3	2.169(2)	N8	C28	1.511(3)
Ni1	N5	2.037(2)	N8	C38	1.479(3)
Ni1	N4	2.023(2)	N7	C35	1.495(3)
Ni2	N6	1.966(2)	N7	C36	1.512(3)
Ni2	N9	2.026(2)	N7	C37	1.486(3)
Ni2	N10	2.031(2)	N5	C20	1.130(4)
Ni2	N8	2.182(2)	N4	C18	1.135(4)
Ni2	N7	2.189(2)	C2	C1	1.390(4)
P1	F1	1.5980(17)	C2	C3	1.395(4)
P1	F4	1.5967(18)	C2	C15	1.505(4)
P1	F5	1.5866(19)	C6	C1	1.396(4)
P1	F2	1.5964(19)	C6	C5	1.392(4)
P1	F3	1.6063(18)	C6	C7	1.500(4)
P1	F6	1.588(2)	C9	C10	1.393(4)
P4	F24	1.586(2)	C9	C8	1.508(4)
P4	F23	1.581(2)	C3	C4	1.388(4)
P4	F19	1.540(3)	C13	C14	1.506(4)
P4	F22	1.535(3)	C13	C12	1.386(4)
P4	F21	1.538(3)	C34	C35	1.511(4)
P4	F20	1.557(3)	C34	C33	1.386(4)
P3	F13	1.6085(18)	C27	C26	1.391(4)
P3	F15	1.6010(19)	C27	C22	1.393(4)
P3	F16	1.5839(19)	C27	C28	1.505(4)
P3	F18	1.605(2)	C26	C25	1.393(4)
P3	F14	1.603(2)	C23	C22	1.393(4)
P3	F17	1.573(2)	C23	C24	1.393(4)
P2	F11	1.584(2)	C23	C36	1.506(4)
P2	F9	1.590(2)	C30	C29	1.505(3)
P2	F10	1.583(3)	C30	C31	1.382(4)
P2	F7	1.577(2)	C5	C4	1.390(4)
P2	F12	1.581(2)	C41	C42	1.456(4)
P2	F8	1.586(3)	C39	C40	1.455(4)
N1	C9	1.335(3)	C18	C19	1.456(4)
N1	C13	1.338(3)	C25	C24	1.394(4)

Atom Atom Length/Å Atom Atom Length/Å

N6	C34	1.338(3)	C10	C11	1.385(5)
N6	C30	1.339(3)	C31	C32	1.389(4)
N9	C41	1.136(3)	C32	C33	1.385(4)
N2	C15	1.510(3)	C12	C11	1.384(5)
N2	C14	1.492(3)	C46	N12	1.136(5)
N2	C16	1.486(3)	C46	C45	1.428(5)
N3	C7	1.508(3)	C44	N11	1.145(5)
N3	C17	1.483(3)	C44	C43	1.452(6)
N3	C8	1.495(3)	C20	C21	1.461(4)

Table S19. Bond angles for 7.

Atom	Atom	Atom	Angle/ ^o	Atom	Atom	Atom	Angle/ ^o
N1	Ni1	N2	81.43(8)	C34	N6	Ni2	119.52(18)
N1	Ni1	N3	81.29(9)	C34	N6	C30	121.8(2)
N1	Ni1	N5	92.98(9)	C30	N6	Ni2	118.64(17)
N1	Ni1	N4	178.53(9)	C41	N9	Ni2	174.1(2)
N3	Ni1	N2	153.92(8)	C15	N2	Ni1	109.13(15)
N5	Ni1	N2	100.98(9)	C14	N2	Ni1	104.22(16)
N5	Ni1	N3	99.28(9)	C14	N2	C15	110.6(2)
N4	Ni1	N2	98.16(9)	C16	N2	Ni1	115.06(17)
N4	Ni1	N3	98.62(9)	C16	N2	C15	108.9(2)
N4	Ni1	N5	88.49(9)	C16	N2	C14	108.9(2)
N6	Ni2	N9	90.95(8)	C7	N3	Ni1	107.76(15)
N6	Ni2	N10	177.01(9)	C17	N3	Ni1	113.28(17)
N6	Ni2	N8	81.17(8)	C17	N3	C7	109.1(2)
N6	Ni2	N7	81.15(8)	C17	N3	C8	110.0(2)
N9	Ni2	N10	91.78(9)	C8	N3	Ni1	106.35(15)
N9	Ni2	N8	99.07(8)	C8	N3	C7	110.3(2)
N9	Ni2	N7	101.75(9)	C39	N10	Ni2	177.2(2)
N10	Ni2	N8	97.19(8)	C29	N8	Ni2	104.56(14)
N10	Ni2	N7	99.47(9)	C29	N8	C28	110.54(19)
N8	Ni2	N7	152.79(8)	C28	N8	Ni2	109.32(15)
F1	P1	F3	179.42(11)	C38	N8	Ni2	115.69(16)
F4	P1	F1	89.42(10)	C38	N8	C29	108.0(2)
F4	P1	F3	90.21(10)	C38	N8	C28	108.61(19)
F5	P1	F1	90.55(11)	C35	N7	Ni2	105.38(15)
F5	P1	F4	90.21(12)	C35	N7	C36	110.0(2)
F5	P1	F2	88.66(12)	C36	N7	Ni2	109.75(16)
F5	P1	F3	89.90(12)	C37	N7	Ni2	114.11(17)
F5	P1	F6	179.06(13)	C37	N7	C35	109.0(2)
F2	P1	F1	90.33(10)	C37	N7	C36	108.6(2)
F2	P1	F4	178.84(13)	C20	N5	Ni1	176.6(2)
F2	P1	F3	90.04(10)	C18	N4	Ni1	175.7(2)
F6	P1	F1	90.39(11)	C1	C2	C3	118.6(2)
F6	P1	F4	89.68(13)	C1	C2	C15	115.0(2)
F6	P1	F2	91.46(14)	C3	C2	C15	125.0(2)
F6	P1	F3	89.16(12)	C1	C6	C7	115.6(2)
F23	P4	F24	178.55(16)	C5	C6	C1	118.7(2)

Atom	Atom	Atom	Angle/°	Atom	Atom	Atom	Angle/°
F19	P4	F24	88.28(16)	C5	C6	C7	124.1(2)
F19	P4	F23	90.62(17)	N1	C9	C10	120.3(3)
F19	P4	F20	89.5(3)	N1	C9	C8	114.6(2)
F22	P4	F24	88.03(16)	C10	C9	C8	125.0(3)
F22	P4	F23	92.90(16)	C2	C1	C6	121.3(2)
F22	P4	F19	89.7(3)	C4	C3	C2	119.6(2)
F22	P4	F21	90.7(3)	N1	C13	C14	114.4(2)
F22	P4	F20	179.2(3)	N1	C13	C12	120.5(3)
F21	P4	F24	91.93(17)	C12	C13	C14	125.1(2)
F21	P4	F23	89.17(17)	N6	C34	C35	114.7(2)
F21	P4	F19	179.5(2)	N6	C34	C33	120.3(2)
F21	P4	F20	90.1(3)	C33	C34	C35	124.8(2)
F20	P4	F24	91.82(17)	C26	C27	C22	118.1(2)
F20	P4	F23	87.23(17)	C26	C27	C28	125.3(2)
F15	P3	F13	179.61(11)	C22	C27	C28	115.7(2)
F15	P3	F18	90.54(11)	C27	C26	C25	119.5(3)
F15	P3	F14	88.67(12)	C22	C23	C24	118.2(3)
F16	P3	F13	90.04(10)	C22	C23	C36	115.2(2)
F16	P3	F15	90.24(11)	C24	C23	C36	125.5(3)
F16	P3	F18	89.32(13)	N6	C30	C29	114.9(2)
F16	P3	F14	176.71(15)	N6	C30	C31	120.7(2)
F18	P3	F13	89.20(10)	C31	C30	C29	124.3(2)
F14	P3	F13	91.03(11)	C4	C5	C6	119.5(2)
F14	P3	F18	87.58(14)	C2	C15	N2	108.4(2)
F17	P3	F13	90.95(11)	N9	C41	C42	179.6(3)
F17	P3	F15	89.31(12)	N7	C35	C34	113.2(2)
F17	P3	F16	91.17(15)	N8	C29	C30	112.5(2)
F17	P3	F18	179.49(16)	N10	C39	C40	178.8(3)
F17	P3	F14	91.92(15)	C6	C7	N3	106.9(2)
F11	P2	F9	91.40(13)	C23	C22	C27	122.2(3)
F11	P2	F8	88.79(16)	N4	C18	C19	179.8(4)
F10	P2	F11	90.86(16)	C26	C25	C24	121.3(3)
F10	P2	F9	90.83(16)	C3	C4	C5	121.0(2)
F10	P2	F8	179.1(2)	C27	C28	N8	108.57(19)
F7	P2	F11	88.26(14)	C11	C10	C9	118.5(3)
F7	P2	F9	179.62(16)	C30	C31	C32	118.3(3)
F7	P2	F10	89.02(17)	N2	C14	C13	112.4(2)

Atom	Atom	Atom	Angle/[°]	Atom	Atom	Atom	Angle/[°]
F7	P2	F12	92.87(16)	C23	C24	C25	119.2(3)
F7	P2	F8	91.80(18)	C33	C32	C31	120.4(3)
F12	P2	F11	178.72(16)	C23	C36	N7	107.6(2)
F12	P2	F9	87.47(15)	N3	C8	C9	112.8(2)
F12	P2	F10	88.56(18)	C32	C33	C34	118.6(3)
F12	P2	F8	91.78(18)	C11	C12	C13	118.5(3)
F8	P2	F9	88.34(16)	C12	C11	C10	120.3(3)
C9	N1	Ni1	119.40(17)	N12	C46	C45	179.7(5)
C9	N1	C13	121.9(2)	N11	C44	C43	178.1(4)
C13	N1	Ni1	118.33(17)	N5	C20	C21	179.7(5)

VIII. References

- 1 D. F. Evans, *J. Chem. Soc.*, 1959, 2003-2005.
- 2 J. Loliger and R. Scheffold, *J. Chem. Educ.*, 1972, **49**, 646-647.
- 3 A. W. Addison, T. N. Rao, J. Reedijk, J. van Rijn and G. C. Verschoor, *J. Chem. Soc., Dalton Trans.*, 1984, 1349-1356.
- 4 L. Yang, D. R. Powell and R. P. Houser, *Dalton Trans.*, 2007, **9**, 955-964.
- 5 C. Magallón, O. Planas, S. Roldán-Gómez, J. M. Luis, A. Company and X. Ribas, *Organometallics*, 2021, **40**, 1195-1200.
- 6 A. J. Wessel, J. W. Schultz, F. Tang, H. Duan and L. M. Mirica, *Org. Biomol. Chem.*, 2017, **15**, 9923-9931.
- 7 1998.
- 8 S. I. Ting, W. L. Williams and A. G. Doyle, *J. Am. Chem. Soc.*, 2022, **144**, 5575-5582.
- 9 W. Zhou, S. A. Zheng, J. W. Schultz, N. P. Rath and L. M. Mirica, *J. Am. Chem. Soc.*, 2016, **138**, 5777-5780.
- 10 W. Zhou, M. B. Watson, S. Zheng, N. P. Rath and L. M. Mirica, *Dalton Trans.*, 2016, **137**, 15886-15893.
- 11 W. Zhou, N. P. Rath and L. M. Mirica, *Dalton Trans.*, 2016, **45**, 8693-8695.
- 12 L. Capdevila, M. T. G. M. Derkx, M. Montilla, J. M. Luis, J. Roithová and X. Ribas, *ChemistryEurope*, 2024, **2**, e202400023.
- 13 A. D. Becke, *J. Chem. Phys.*, 1993, **98**, 5648-5652.
- 14 C. T. Lee, W. T. Yang and R. G. Parr, *Phys. Rev. B: Condens. Matter Mater. Phys.*, 1988, **37**, 785-789.
- 15 F. Weigend and R. Ahlrichs, *Phys. Chem. Chem. Phys.*, 2005, **7**, 3297-3305.
- 16 F. Weigend, *Phys. Chem. Chem. Phys.*, 2006, **8**, 1057-1065.
- 17 M. J. T. Frisch, G. W.; Schlegel, H. B.; Scuseria, G. E.; Robb, M. A.; Cheeseman, J. R.; Scalmani, G.; Barone, V.; Petersson, G. A.; Nakatsuji, H.; Li, X.; Caricato, M.; Marenich, A. V.; Bloino, J.; Janesko, B. G.; Gomperts, R.; Mennucci, B.; Hratchian, H. P.; Ortiz, J. V.; Izmaylov, A. F.; Sonnenberg, J. L.; Williams-Young, D.; Ding, F.; Lipparini, F.; Egidi, F.; Goings, J.; Peng, B.; Petrone, A.; Henderson, T.; Ranasinghe, D.; Zakrzewski, V. G.; Gao, J.; Rega, N.; Zheng, G.; Liang, W.; Hada, M.; Ehara, M.; Toyota, K.; Fukuda, R.; Hasegawa, J.; Ishida, M.; Nakajima, T.; Honda, Y.; Kitao, O.; Nakai, H.; Vreven, T.; Throssell, K.; Montgomery, J. A., Jr.; Peralta, J. E.; Ogliaro, F.; Bearpark, M. J.; Heyd, J. J.; Brothers, E. N.; Kudin, K. N.; Staroverov, V. N.; Keith, T. A.; Kobayashi, R.; Normand, J.; Raghavachari, K.; Rendell, A. P.; Burant, J. C.; Iyengar, S. S.; Tomasi, J.; Cossi, M.; Millam, J. M.; Klene, M.; Adamo, C.; Cammi, R.; Ochterski, J. W.; Martin, R. L.; Morokuma, K.; Farkas, O.; Foresman, J. B.; Fox, D. J., Gaussian 16, Revision C.01, *Gaussian, Inc.*, Wallingford CT, 2016.
- 18 Bruker, APEXIII. Bruker AXS, Inc., *Madison, Wisconsin, USA*, 2018.
- 19 G. Sheldrick, A short history of SHELX, *Acta Cryst. A: Found. Cryst.*, 2008, **64**, 112-122.
- 20 G. Sheldrick, SHELXT - Integrated space-group and crystal-structure determination, *Acta Cryst. Sec. A*, 2015, **71**, 3-8.
- 21 O. V. Dolomanov, L. J. Bourhis, R. J. Gildea, J. A. K. Howard and H. Puschmann, *J. Appl. Crystallogr.*, 2009, **42**, 339-341.